2013

INVESTIGATING THE POTENTIAL APPLICATIONS OF A RAMAN TWEEZER SYSTEM

John Wray
Virginia Commonwealth University

INVESTIGATING THE POTENTIAL APPLICATIONS OF A RAMAN TWEEZER SYSTEM

A thesis submitted in partial fulfillment of the requirements for the degree of Master of Science at Virginia Commonwealth University.

by

John Casey Wray
Bachelor of Science Physics
Minor: Chemistry
Minor: Mathematical Sciences
Virginia Commonwealth University, May 2011

Director: Joseph E. Reiner, Assistant Professor, Department of Physics

Virginia Commonwealth University
Richmond, Virginia
May, 2013

Acknowledgement

First, I would like to acknowledge Professor Joseph E. Reiner for allowing me to work with him during my time in the Physics Graduate Program here at VCU. Furthermore, I would like to thank him for providing the equipment as well as the knowledge was necessary to perform the experiments discussed in this thesis.

Also, I would like to acknowledge Professor Massimo Bertino for sharing his lab and providing the Area upon which this setup was constructed. I would like to thank him for providing the aggregates used for SERs enhancement and for aiding in using the newly encountered instrumentation (i.e. the Raman detector).

Lastly, I wish to acknowledge those serving on the committee for taking the time to listen to my Thesis Defense and read the Thesis provided here. Thank You for allowing me this opportunity to contribute my knowledge to the scientific community and those who inquire.

TABLE OF CONTENTS

List of Figures

List of Abbreviations

Ag	Silver
AR	Anti-Reflective
CW	Continuous Wave
IR	Infrared
NA	Numerical Aperture
ND	Neutral Density
OD	Optical Density
OT	Optical Tweezer
SERs	Surface-Enhanced Raman Scattering

List of Symbols

F	Force
μ	Dipole
μ_{ind}	induced Dipole
$\mathcal{E}$	Electric Field
E	Energy
ν	Frequency
p	Momentum
nm	nanometer
h	Planck's Constant
α	Polarizability
c	Speed of Light
t	Time
λ	Wavelength

Abstract

INVESTIGATING THE POTENTIAL APPLICATIONS OF A RAMAN TWEEZER SYSTEM

By John C. Wray, B.S. Physics.

A thesis submitted in partial fulfillment of the requirements for the degree of Master of Science at Virginia Commonwealth University.

Virginia Commonwealth University, 2013.

Major Director: Joseph E. Reiner, Assistant Professor, Department of Physics

This thesis describes the construction of an Optical Tweezer apparatus to be used in conjunction with a confocal Raman spectrometer. The tweezer utilizes an infrared (λ=1064 nm) laser directed into an inverted microscope with NA=1.4 oil immersion 100x objective lens that strongly focuses the laser light into a sample to function as a single-beam gradient force trap. The long term goal of this research program is to develop a single molecule Raman tweezers apparatus that allows one to control the position of a Raman nanoplasmonic amplifier. This thesis describes the construction of the Raman tweezer apparatus along with several Raman spectra obtained from optically trapped samples of polystyrene fluorescent orange, amine-modified latex beads. In addition, I explored the Raman spectra of bulk cytochrome c mixed with or injected onto Ag aggregates for SERs enhancement.

1. Introduction

1.1 Motivation

The goal of this research project was to improve Raman spectroscopic techniques by designing an experimental system that controls the position of a Raman nanoplasmonic amplifier for single molecule sensitivity. More specifically, we have built a Raman Tweezer system to allow one to position the nanoplasmonic amplifier at a predetermined location. A setup for a Raman Tweezer is described using highly focused laser beams to trap, manipulate, and position particles with high precision while simultaneously performing Raman scattering spectroscopy on the trapped particles.

Raman scattering is very weak and difficulties arise when attempting to perform experiments at the single molecule limit. Raman spectroscopy involves studying the interaction of electromagnetic radiation with matter and is a very powerful technique. Raman scattering spectroscopy is a popular analytical tool that is noninvasive to samples, non-destructive in nature, allows for rapid spectral measurements, identifies composition and structure of particles, and probes the particles chemistry and reactivity. The drawbacks of Raman spectroscopy are that Raman scattering cross sections are very weak which leads to low sensitivity in measurements and interference from solution or other matter. In addition, Brownian motion of the particles also limits the quality of the spectral data. Optical Tweezers use highly focused laser beams that trap and manipulate dielectric or metallic particles that range in size from 50 nm to10 μm. Optical tweezers are a unique, noninvasive technique providing a method to trap and manipulate

microscale objects without requiring direct contact with the object; hence, optical tweezers are found to be considerably useful in analytical applications involving characterization of materials. The Raman tweezer is a technological development that involves combining optical tweezers and Raman scattering spectroscopy and introduces a vibrational spectroscopy tool into numerous fields for particle analysis. Optical tweezers combined with Raman scattering spectroscopy greatly reduces the undesirable effect from the inevitable Brownian motion on the Raman spectra and allow high-resolution measurements to be obtained from the Raman spectra of optically-immobilized particles.

2. Background Information

2.1 Optical Tweezers

Light has momentum, as well as energy and is capable of exerting a mechanical force on matter. The principle of the conservation of momentum shows that when light is reflected, refracted, or absorbed by a particle it undergoes a change in momentum; analogously, this interaction results in the particle experiencing a change in momentum, i.e. a resulting force. Optical tweezers emerged in the technological developments from the historical demonstrations exploiting the ability for light to exert a mechanical force on matter. An optical tweezer is an experimental technique that involves optically manipulating and trapping individual particles in three-dimensions using a single, highly-focused laser beam without requiring direct contact.

In 1970, Arthur Ashkin pioneered the entire field of optical manipulation after reporting the first observation of accelerating and trapping of freely suspended, micron-sized particles in stable optical potential wells using only the force of radiation pressure from continuous-wave visible laser light.[1] He discovered that optical forces responsible for particle trapping can be decomposed into two individual components: a scattering force and a gradient force. The scattering force is proportional to the light intensity and is in the direction of light propagation, and the gradient force is proportional to the spatial gradient in light intensity and acts in the direction of the spatial gradient. In 1986, Ashkin et al. reported the first experimental observations of a single-beam gradient force radiation-pressure particle trap discovering the optical tweezer.[2] The optical tweezer was the first all-optical single-beam trap using only a

strongly focused beam in which the axial gradient force is so large that it dominates the scattering force; hence, particles were trapped three-dimensionally in both the plane transverse to the laser beam propagation and in the axial direction.[2]

When the trapped particle diameter *d* is much larger than the wavelength λ ($d \gg \lambda$) of the trapping laser, the conditions for Mie scattering are satisfied and a simple ray-optic model can be used to explain, understand, and compute the optical forces brought about by changes in momentum of scattered and refracted radiation.[2-6] In the Mie scattering regime, diffraction effects are neglected and the rays both reflect and refract at the surface of the particle causing momentum to transfer from the trapping laser to the interacting particle; consequently, this produces an optical force described by Newton's second and third laws.[7] Specifically, the rate of change of the momentum in the deflected rays conveys an equal and opposite rate of change in the momentum to the particle; hence, the time rate of change of the momentum is the trapping force exerted on a particle.[4,5,8-11]

FIGURE 2.1.1 illustrates the principal of trapping in the radial and axial directions. For radial trapping an incoming beam of unfocused light with a Gaussian intensity profile is shown. If the bead has a higher index of refraction than the surrounding medium, then the light rays will obey Snell's law ($n_1 \sin\theta_1 = n_2 \sin\theta_2$) in the manner shown. The rays will refract at both interfaces and this refraction results in a momentum change for the light ray.[7,11] According to Newton's 2nd Law of motion this can be thought of as the bead exerting a force on the light which results in a change in the momentum of light. From, Newton's 3rd Law of motion we know that the light ray will also exert an equal and opposite force back on the bead. Given the Gaussian intensity profile we can see that if the bead is displaced from the center of the incoming beam, then there will be a net force that is exerted on the bead. This results in the bead

experiencing a restoring force to the center of the incoming Gaussian beam. A similar analysis can be performed for the axial trapping direction. In both cases it is clear that the particle will experience a restoring force to the center of the focus of the incoming ray.

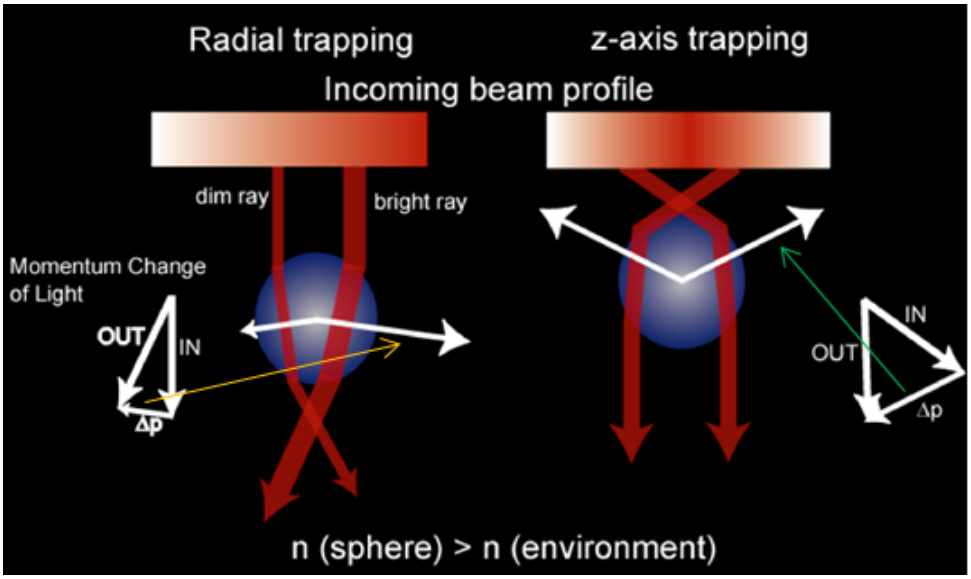

FIGURE 2.1.1: A schematic illustration of the ray-optics explanation for optical trapping. Radial trapping (left) and axial trapping (right) can be understand by ray tracing through Snell's Law and Newton's 2nd and 3rd laws of motion. For the radial trapping we see two incoming rays from above the bead and both rays are refracted as they travel through the particle. The momentum change in the light of the bright ray is shown as white vectors and from Newton's 3rd law we know the light exerts the opposite momentum change on the particle (orange arrow is meant to indicate the connection between the momentum change of the light and the force applied on the sphere). For trapping in the z-axis we note that the incoming ray must be highly focused, but the principle is the same, the rays are refracted, which leads to a change in momentum. This change in momentum of the light leads to a momentum change imparted onto the bead (green arrow). If the bead is at the center of the focus, then the combination of the forces on the particle will force the particle upwards towards the center of the focused light.

Again, this ray-optics explanation is only valid for particle diameter much larger than the wavelength of the trapping light, $\lambda \gg d$. Even though the analysis for a particle where $\lambda \sim d$ has no known closed form description and is beyond the scope of this thesis, it has been demonstrated that particles can be optically trapped over a broad range of sizes. The important message is that the particle you are trying to trap must have an index of refraction greater than the surrounding medium and the particle will be attracted to the focus of a high NA microscope

objective.[9] Finally, high NA immersion lenses are required in order to stably trap particles in three-dimensions.[2,7-10] The optical trapping reported in this thesis satisfies all these conditions.

2.2 Raman Scattering Spectroscopy

C.V. Raman became interested in the phenomenon of light scattering on a boat trip from England to India when he noticed that he could not remove the blue reflected light from seawater at the Brewster angle when using a Nicole prism.[12] This led him to conclude that the blue color must appear as a consequence of scattering from the water and this prediction inspired him to perform a course of experiments with his students investigating this effect over the next seven years. After initial rejection from the reviewer at the journal of *Nature*, the results he submitted were finally published in a 1928 article titled *A New Type of Secondary Radiation.* His experiments led him to the discovery of a new field of optical spectroscopy and he was awarded the Nobel Prize in 1930.[12,13] Raman spectroscopy research was relatively quiet until the invention of the laser in the 1960s. Ultimately, the availability of the laser as an excitation source ushered a new period of Raman spectroscopy because of the unprecedented power and intensity made available with the invention of the laser replacing the inefficient, outdated instruments.

In Raman spectroscopy, light of a single frequency ν, is focused onto a sample, and only the scattered non-resonant light is observed. Light generally transmits through most Raman samples unscattered while some (~0.1%) undergoes Rayleigh scattering,[12-14] which is an on-resonance phenomenon. A very small fraction (<<0.1%) of the scattered light is found to be off-resonance. This light originates from a process called Raman scattering.[12-14] The Raman scattered frequency ν_i may be greater than or less than ν, but the amount of light with frequency $\nu_i < \nu$ known as Stokes radiation[12-14] is much greater than the amount of light with frequency $\nu_i > \nu$ known as anti-Stokes radiation.[12-14]

Scattering originates from the interaction between incident light and sample such that energy is conserved and $\Delta E = h|\nu - \nu_i|$ corresponds to the energies that are absorbed by the

sample.[12-14] In Raman spectroscopy, light of greater than IR frequencies is used and we measure the differences,$|\nu - \nu_i|$ between the Raman scattered light and the incident light.[12-15] In most cases, ΔE is an innate property of the system and is independent of the frequency of the incident light; thus, the Raman frequency $\nu - \nu_i$ must also be independent of the frequency of the incident light. One can use classical theory to demonstrate that the absolute value of the Stokes frequency equals that of the anti-Stokes frequency.[12-15]

A dipole moment, μ_{ind}, is induced in a molecule placed within an external electric field, $\mathcal{E}$ that is proportional the field strength, $\mu_{ind} = \alpha\mathcal{E}$; hence, the proportionality constant α,is the molecular polarizability that is physically related to the extent the external field is able to disturb the electron density of the molecule out of its equilibrium configuration.[13-15] The real part of the oscillating electric field can be expressed as $\varepsilon = \varepsilon_o \cos(2\pi\nu t)$, and the polarizability, α, can be given as $\alpha = \alpha_o + (\Delta\alpha)\cos(2\pi\nu_0 t)$, its magnitude has maximum variation (Δα) from the equilibrium polarizability (α_0) at the natural vibrational frequency (ν_0) of the bond in an oscillating molecule.[13,14,15] Consequently, find that the equation[13]

$$\mu_{ind} = \alpha_0\mathcal{E}_0 \cos 2\pi\nu t + \frac{1}{2}(\Delta\alpha)\mathcal{E}_0[\cos 2\pi(\nu + \nu_0)t + \cos 2\pi(\nu - \nu_0)t]$$

predicts that the induced dipole moment will oscillate with components of frequency ν, $\nu + \nu_0$, and $\nu - \nu_0$.[13-15] The first term oscillates at the same frequency as the incident radiation and thus will be responsible for scattered light at the frequency, i.e., elastic Rayleigh scattering.[14] The time dependence of the second term represents a source for radiation, which is blue-shifted[14] with respect to the laser frequency. This so-called anti-Stokes scattering is identical to the Stokes spectrum, but has a strongly reduced intensity due to the Boltzmann factor that describes the population of the thermally excited vibrational states. The third term is the red-shifted[14] inelastic

scattering term that contains information about the molecular system via dependence on ν_0. It is the source of the Stokes scattering that is usually presented as the Raman spectrum.

Derivations of the intensities observed in a Raman spectroscopic experiment are beyond the scope of this thesis. The important points are that the intensity of Raman scattering is very weak and usually amounts to 10^{-12}~$10^{-6}$of the incident light and the inelastic scattering cross sections are small with $\sigma \sim 2\times10^{-28}$ cm^2.[9] To overcome this weak scattering cross section, most Raman spectra are performed on bulk samples with $> 10^{20}$ or so molecules in the excitation beam volume. To get better sensitivity one needs to reduce the excitation volume and excite the smaller size sample with higher intensity light.[12-14] This has been achieved through the development of confocal Raman microscopy.[14]

2.3 Confocal Raman Microscopy

In confocal microscopy, a point-like source (i.e. laser) is focused with an objective onto a sample.[14] The spatial extension of the focal spot on the sample is determined by the wavelength λ, the numerical aperture of the objective, and the degree to which the back aperture of the objective is filled by the incoming laser light. Back-scattered light from the sample is then focused through the same (or a second) lens onto an aperture (pinhole) in front of a detector. The size of the pinhole is chosen so that only the central part of the focus can pass through the pinhole and reach the detector. The pinhole diameter is crucial in obtaining the highest depth resolution as well as optimizing collection efficiencies, because the Raman signal is typically very weak. The illuminating point source and the pinhole are both positioned in confocal imaging planes. Signal is detected through the pinhole only from light originating from the focal plane; therefore, scattered light from above or below the focal point does not contribute to the image. From this simple geometrical representation, two advantages of confocal microscopy can already be seen: a three-dimensional image of the sample can be obtained and image contrast is strongly enhanced.

Problems arising from the weak Raman effects can be overcome by carrying out the Raman scattering measurement in a confocal microscope, where a small detection volume is defined by the focused excitation laser beam and by imaging the collected scattering through a matched aperture.[14] This detection volume is generally diffraction limited and small (~1 fl) and can be filled with a single particle in dilute dispersions.[9] The resulting measurements provide local composition information about the particle, changes in which may be related to chemical reactions or exchange of bound molecules with the surrounding solution.[9] Another enhancement mechanism for Raman microscopy is surface-enhanced scattering.[14]

2.4 Surface-Enhanced Raman Spectroscopy

Further enhancement of the Raman signal has been achieved with the advent of enhanced electric fields resulting from the coupling of light to plasmonics resonances in certain metals. Surface-enhanced Raman spectroscopy (SERS) was first observed by *Fleischman* et al. in 1974,[14,16] and discovered by Jeanmarie and Van Duyne and Albrecht and Creighton in 1977.[16] It has been shown earlier in the 1970s that the Raman signal is enhanced when molecules were adsorbed onto specific substrates. The localized fields due to surface plasmon resonance and chemical effects were found to cause SERS enhancement. The field enhancement associated with surface plasmons has been extensively investigated as a means for increasing the interaction strength between a molecule and optical radiation.

In the case of surface-enhanced Raman scattering, the molecular species is brought into close contact with a roughened or nanoengineered metallic surface, which increases the Raman scattering cross-section by 15 orders of magnitude.[14] Essentially, enhancement of Raman-scattering cross-sections is sometimes observed for samples supported on roughened or corrugated surfaces (typically silver is used).[15] This degree of enhancement allows for single molecule Raman spectroscopy.[14] Two mechanisms are considered to account for the SERs effect: (1) an electromagnetic mechanism for an enhancement of the electric field $\mathcal{E}$ and (2) a chemical mechanism for a chemical enhancement originating in the surface-induced changes of the molecular polarizability α.[14]

2.5 Raman Tweezers

More recently, groups have begun to combine optical tweezers with a Raman spectrometer in the hope of isolating individual particles for Raman and SERs detection. The acquisition of a Raman spectrum of an optically trapped particle provides chemical analysis of single colloid particles in solution. In addition, by trapping metallic nanoparticles and aggregates of nanoparticles, it has been shown that optical tweezers can be combined with SERs to approach single molecule Raman scattering measurements of optically trapped particles. The optical tweezer provides a means for the experiments to move the nanoplasmonic particle or trapped colloidal particle to different points in a sample and thus study the effects of different regions or environments and their effect on the Raman spectra. In addition, one can imagine optical tweezers in conjunction with Raman spectroscopy setting the foundation to achieve a higher degree of accuracy when quantifying the number and types of molecules that actually interact with a SERs amplifier.

3. Applications

A single tightly focused laser beam that traps, in three dimensions a microscopic particle near the beam focus has become established as a powerful non-invasive technique known as an *optical tweezer*.[11] Optical Tweezers are routinely applied to measure the elasticity, force, torsion, and position of a trapped object.[11] Optical tweezers have trapped dielectric particles in the size range from 10 μm down to ~25 nm were stably trapped in water solutions; applied to individual colloidal particles in water.[2] In biological applications of optical trapping and manipulation, it is possible to remotely apply controlled forces on living cells, and large biological molecules without inflicting detectable optical damage.[4] Piconewton forces and micrometer length scales make optical tweezers a perfect tool to study the range of microscopic phenomena, from colloidal physics to molecular biology.[10]

Optical Tweezers can be used to trap and manipulate matter and are useful in applications for building nanomaterials and nanodevices. Optical Tweezers have found numerous applications (i.e. measuring forces and motion) in the fields of biophysics, nanotechnology and the nanosciences performing nanomechanical measurements on macromolecules and their assemblies.

Raman scattering spectroscopy provides a nearly ideal tool for investigating the chemical structure of colloidal particle dispersions.[9] Raman scattering with water is weak, the technique is compatible with aqueous solutions typically used for particle dispersions.[9] Despite the achievements Raman scattering spectroscopy there are limitations to single-particle

measurements; however, Raman Tweezers can provide molecular structure information on the composition and reactivity of individual suspended particles, and it has been applied to emulsion chemistry, material analysis, solid-phase synthesis, liposomes, biotechnology, and clinical assays.[9] Single particles can be trapped and microchemical analysis can be performed using Raman spectroscopy.[9] Coupling Raman Tweezers to other detection based devices have potential applications in enhancing Raman signal for sample analysis that could allow new properties and processes to be discovered in materials.[9] Single particles can be trapped and analyzed from small-volume (submicroliter) samples of very dilute (10^6 particles ml^{-1}) dispersions.[9]

Surface-Enhanced Raman spectroscopy can be used as an enhancement mechanism for Raman microscopy allowing for the detection of Raman signals from single molecules.[14]

The combination optical trapping of small particles with Raman spectroscopy can be used to provide molecular structure information about individual, femtogram-sized particles in liquid samples. Increased focus has been placed upon the application of optical-trapping confocal microscopy to particulate samples in liquids.

4. Experimental

4.1 Materials

This experiment was constructed on an 8×4 ft^2 optical table with advanced vibration isolation features. An infrared ($\lambda = 1064\ nm$) laser beam, 700 mW, (CrystaLaser) was used for trapping, and a continuous-wave visible (λ = 532nm) laser (coherent) beam with adjustable power was used for performing Raman spectroscopy. An inverted microscope (Zeiss) with a NA 1.4 oil-immersion 100x objective lens (Zeiss) was equipped with a steel, 3-axis, XYZ-translation stage with 100 *nm* resolution (Thorlabs) offered stability positioning capabilities. Bright field illumination was provided with a LED light Source (Thorlabs) and visualization of the trapping was attain by externally attaching a camera (Sony) connected to a monitor (Dell) to the microscope.

Various mirrors (New Focus), lenses (Newport), and optomechanical components (Thorlabs) were used to direct the laser beams into the microscope to focus laser light into the solution. These components included manual filter wheel for filters, fixed lens mounts and mirror mounts, and kinematic mirror mounts. Kinematic mirror mount simplified beam alignment and allowed precision control for manipulation of trapped objects. Other components included flat mirrors, convex lenses, dichroic mirror/beam splitters, and neutral density (ND) filters. The dichroic mirror (Thorlabs) was rated to be 90%/10% reflection/transmittance at 1064 nm and 532 nm and the neutral density (ND) filters with OD:1 and OD:3 were anti-reflective (AR) coated to attenuate the power of the incoming laser beams.

A XenoWorks Digital Microinjector (Sutter) was used to inject cytochrome c into sample solution and a Raman spectrometer (Jobin) was used to obtain Raman spectra. Additional optomechanical components included fluorescence imaging filters and a fluorescence filter cube. The samples were prepared on a glass slide with a 1 cm hole drilled through the center. Two 1.5 coverslips were attached to the top and bottom of the slides to seal the hole and created a 100 μL well for solutions. All samples were dissolved in aqueous solutions. The sample solutions included 1 micron diameter polystyrene fluorescent orange, 2 micron diameter amine-modified latex beads and bulk cytochrome c mixed with or injected onto Ag aggregates. The Ag aggregates were provided by Prof. Massimo Bertino (VCU Physics) and they were formed through a pulsed laser protocol developed in his lab. The Ag nanoparticles remained stable over a period of several months during the time frame of the experiments reported here.

4.2 Raman Tweezer Setup

The Raman tweezer setup is illustrated by the schematic shown in **Figure 4.2.1**. The infrared (1064 *nm*) trapping laser was overlapped with the continuous-wave, visible (532 *nm*) Raman laser by positioning a dichroic mirror in the optical path in order to transmit the Raman laser while simultaneously reflecting the trapping laser; thus, both beams were focused into the back aperture of the microscope objective.

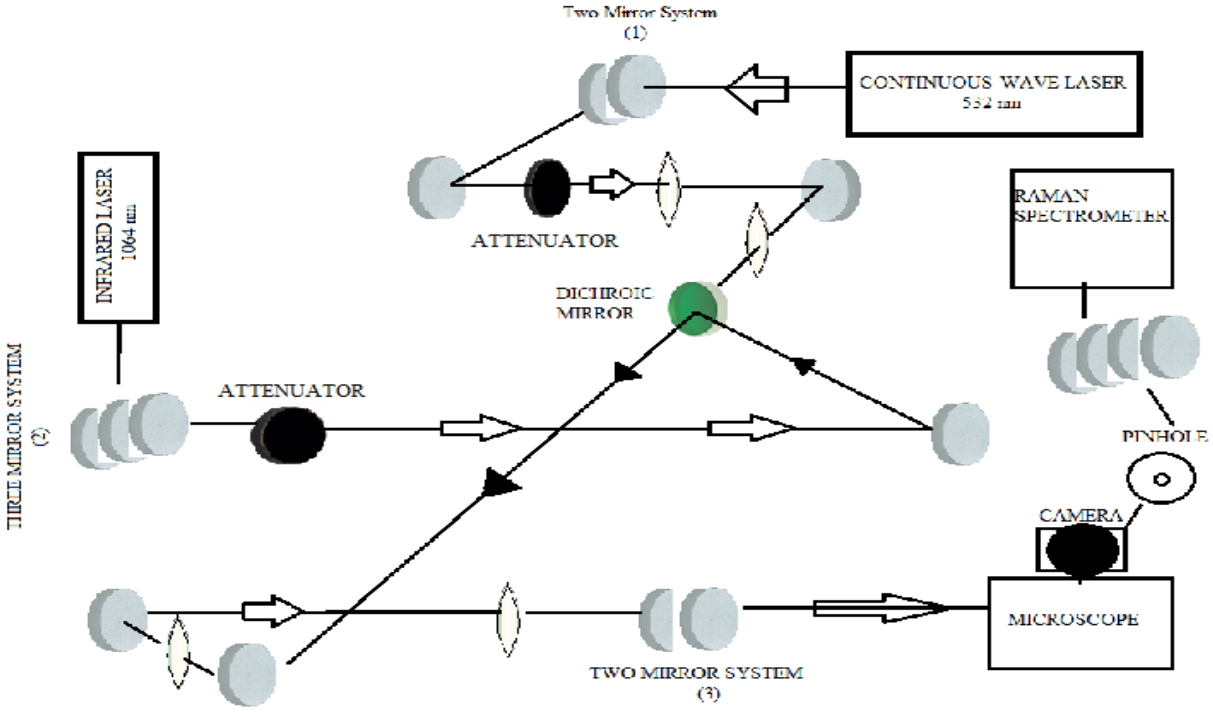

FIGURE 4.2. 1: Schematic of the constructed Raman tweezer.

In the above schematic, (1) a two mirror periscope was used to raise the visible (532 nm) laser beam to the same height as the other optomechanical components, (2) another two mirror periscope and a third mirror raised and launched the infrared (1064 nm) laser to the same height as the visible laser, and (3) a third two mirror periscope was used to raise the two overlapped laser beams and direct them into the microscope to be focused into the sample solution. The attenuator for the infrared laser was mounted on a filter wheel that included an OD 1.0 and an

OD 3.0 neutral density filter. All the mirrors were flat mirrors and were mounted on kinematic mirror mounts that simplified beam alignment and allowed precision control for manipulation of trapped objects. The dichroic mirror allowed the green laser to be overlapped with the infrared laser. A manipulator was placed for a 75 μm pinhole that will be included in future experiments. In addition, fluorescence filters were placed in front of the detector to filter light that came from the microscope and the mirrors were used to direct the filtered light into the Raman spectrometer.

4.3 Calibration and Methodology

Construction of the Raman Tweezer system began with assessing the space limitations of the shared optical table and designing a layout for the setup to properly determine where to position the lasers, the optomechanical components, the microscope, and the Raman spectrometer. First, the visible (532 *nm*) laser and the infrared (1064 *nm*) laser were individually mounted and positioned in different areas on the optical table. Secondly, multiple flat mirrors were independently positioned in front of each laser source in order for both of the emitted laser beams to be raised to equal heights above the optical table. Next, an attenuator was positioned in the optical path of each laser to reduce the optical intensity of the beams to prevent optical damage to sample particles from occurring. A dichroic mirror was positioned in the optical path to overlap the transmitted visible (532 *nm*) laser beam with the reflected infrared (1064 *nm*) laser beam.

The placement of two 10 *cm* lenses were positioned in the optical path of only the visible (532 *nm*) laser to focus the beam at infinity as it was transmitted through the dichroic mirror and overlapped with the infrared (1064 *nm*) laser. The optimal position for each lens was found from calculations using the thin lens equation: $\frac{1}{q_o} + \frac{1}{q_i} = \frac{1}{f}$, where q_o is the object distance, q_i is the image distance, and *f* is the focal length of the lens. This equation was used to determine the position of a 50.0 *cm* lens and the 15.0 *cm* lens placed in the optical path of both the overlapped lasers. Flat mirrors were placed to direct the focused light from the lenses into the microscope to be highly focused into a sample solution.

A one-inch hollow tube was mounted onto the RMS threading of the inverted microscope and used to aid in the alignment of the incoming light through the microscope. Briefly, we used a two point method for aligning the beams in the following way, all lenses were removed from the

optical path (including the objective) and we centered the incoming beams on the center of the objective mount using the mirror farthest from the microscope. Then we would attach the one-inch tube to the objective mount and center the two beams at a distance of (10~12 inches) above the objective mount with the near mirrors in the optical train. This process of *walking* the beam was repeated until the beam was centered at both locations defined by the tube, this ensured that the incoming beam was centered on the back aperture of the microscope objective; furthermore, this guaranteed the beams would be aligned and overlapped. A camera was attached external to the microscope to visually observe further refinements to the two beams and similar adjustments were made with the two sets of the previously described mirrors until both beams were overlapped and focused at the same spot in the sample. Finally, all lenses were placed in the optical path and the beams overlap was recovered by making sure the beams went through the center of each lens.

Fluorescent orange, polystyrene beads (Sigma) that are characterized by their green/fluorescent orange excitations were diluted by a factor of 1000 and freely suspended in milli-Q water. Added 100 μL of this diluted solution to the glass slide and positioned it on top of the microscope objective. Observing trapping of the polystyrene beads was conveniently straightforward when using the high NA microscope objective. The positions of the lenses were changed to move the focus of the beam in the sample and successfully trap polystyrene beads and observe fluorescence simultaneously. We optimized the fluorescence spectra by adjusting the alignment of the trap and Raman excitation lasers.

Ag aggregates were formed to create SERs hot spots with cytochrome c detection. Aggregation was initiated by mixing a 1M KCl/Ag cluster solution in a 1:1 ratio and then mixed 0.1 mg bulk cytochrome c. Slide was prepared by adding 100 μL Ag/cytochrome c solution. Ag

aggregates were also formed without the addition of cytochrome c in order to demonstrate controlled loading of cytochrome c molecules onto the Ag hotspots formed in the Ag aggregates. Again, aggregation was initiated by mixing 1M KCl/Ag clusters in a 1:1 ratio and a slide was prepared using 100 μL of this solution. Loaded Ag aggregates with bulk cytochrome c by direct injection onto the Ag aggregates using the XenoWorks Digital Microinjector.

5. Results

Experiments were performed on individual colloidal polystyrene latex beads in water and the constructed Raman tweezer apparatus successfully trapped beads and observed their fluorescence. The laser beams were attenuated to decrease optical intensities to prevent optical damage to the samples. The rate of photobleaching decreased with decreased powers. and observed their Raman spectra; furthermore, the Raman spectra of cytochrome c was observed. Figure 5.1, Figure 5.2, and Figure 5.3 show the Raman spectra of the objective only, glass coverslip, and a slide with only water respectively. Figure 5.4, Figure 5.5 and Figure 5.6 all show the Raman spectra of a trapped polystyrene bead. Figure 5.7 and Figure 5.8 show the Raman spectra of the Ag/cytochrome solution. Figure 5.9 show the Raman spectra of cytochrome c microinjected onto the hotspots of the Ag clusters. The equation to convert the Raman wavelength to the wavenumber was

$$\Delta\omega = \left(\frac{1}{532.1\ [nm]} - \frac{1}{\lambda\ [nm]}\right) \times 10^7\ \ [cm^{-1}]$$

The captured Raman spectrum of the polystyrene beads shows peaks to be around 1000 cm^{-1}. We showed the injector could be used to increase the Raman signal and showed evidence that we were successfully loading cytochrome c onto the hot spots of the Ag aggregates. The spectra for SERs showed very sharp peaks.

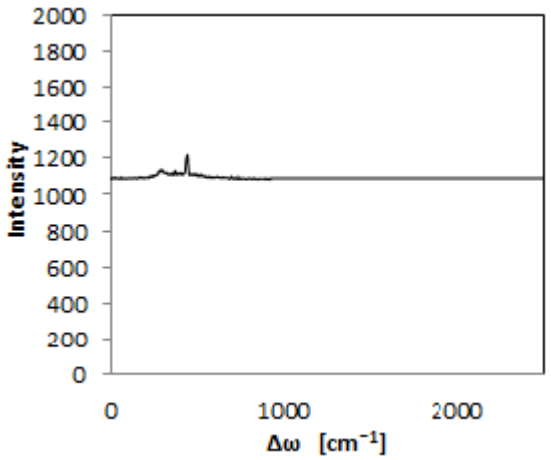

FIGURE 5.1: Raman 532 nm 20 mW Objective Only

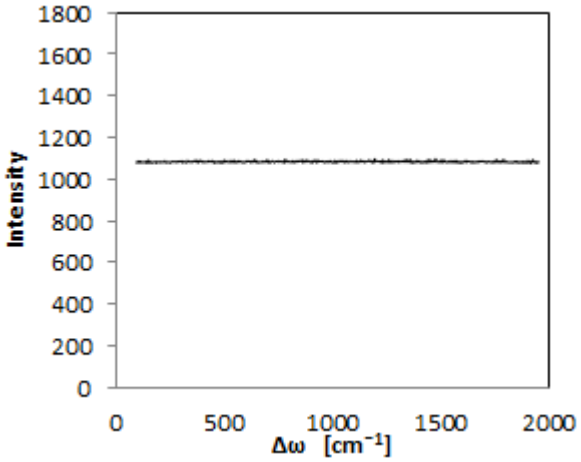

FIGURE 5.2: Raman 532 nm 9.4 mW Glass Coverslip

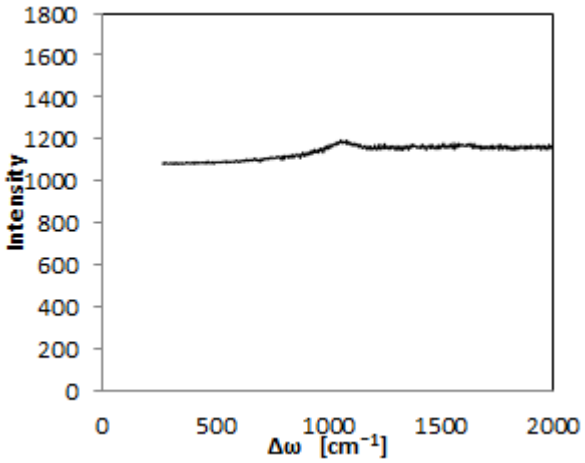

FIGURE 5.3: Raman 532 nm 33.5 mW Glass Coverslip and Water

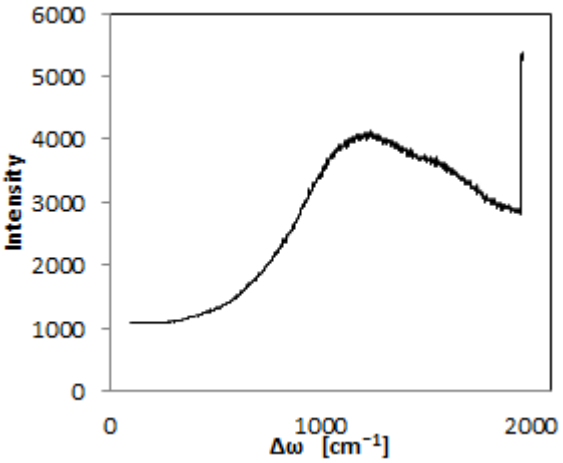

FIGURE 5.4: Fluorescence 532 nm 60 mW Polystyrene Beads

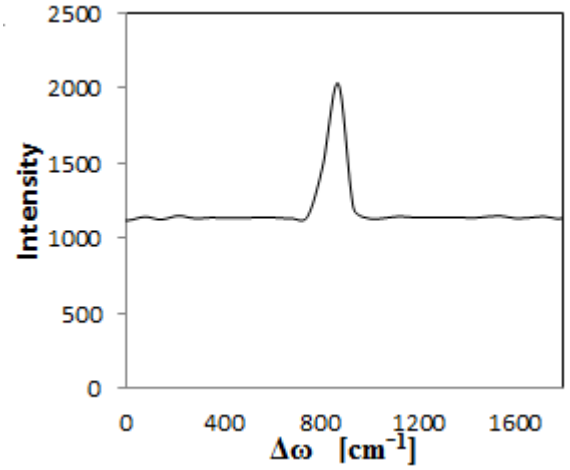

FIGURE 5.5: Raman 532 nm 33.5mW Polystyrene Bead

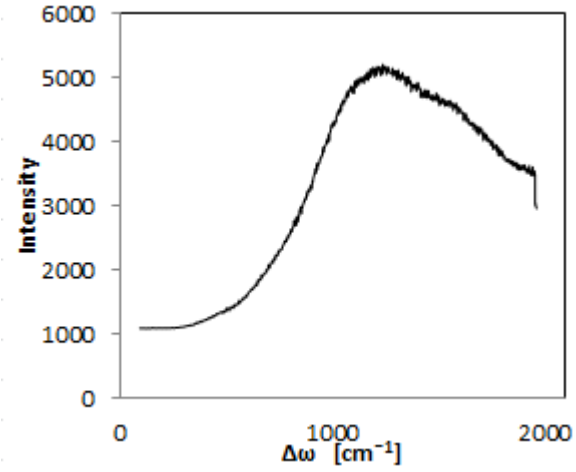

FIGURE 5.6: Fluorescence 532 nm 60 mW Polystyrene Bead

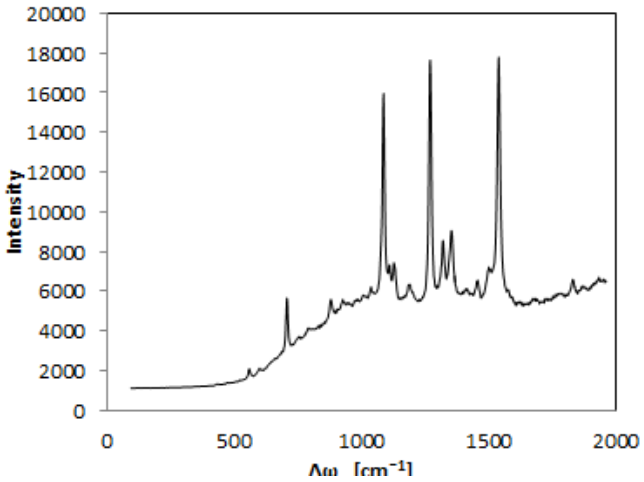

FIGURE 5.7: Raman 532 nm
1 mW incoming light 16 µW excitation
100 µL Cytochrome C Solution
premixed with Ag nanoparticles.

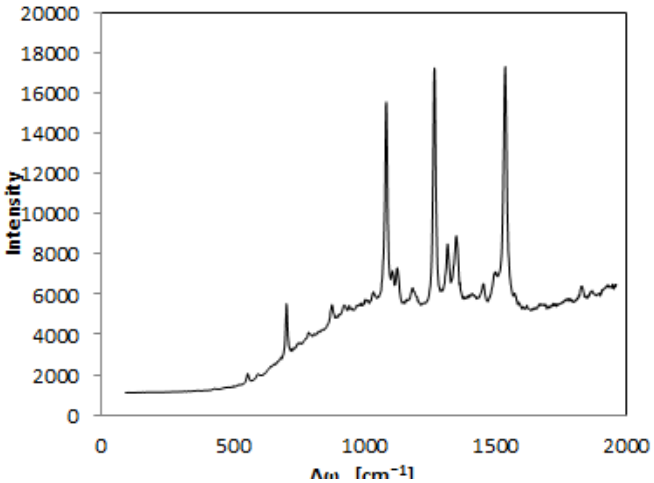

FIGURE 5.8: Raman 532 nm
1 mW incoming light 16 µW excitation
100 µL Cytochrome C Solution
premixed with Ag nanoparticles.

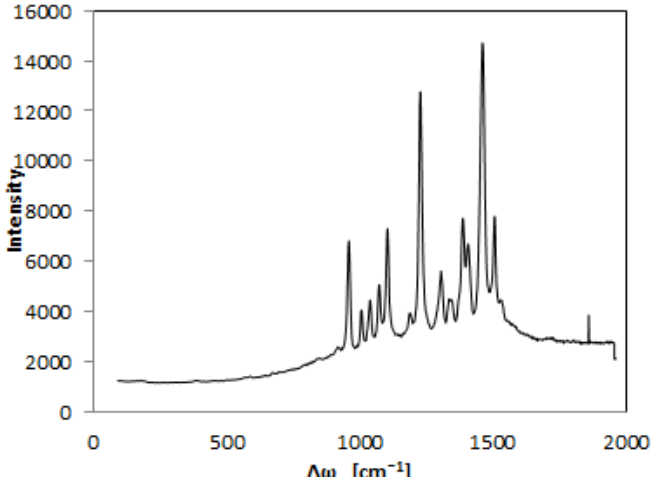

FIGURE 5.9: Raman 532 nm 5.8mW
100 µL Ag/KCl Solution Cytochrome C
microinjected on hot spots

6. Discussion

Built Raman Tweezer setup with an infrared trapping laser (λ=1064nm) overlapped with a green Raman laser (λ=532nm) that was directed into an inverted microscope using 100x objective lenses with NA=1.4 to focus the light into solution. Immersol 518F was used for an oil immersion to achieve the increased resolution of the microscope. This experiment demonstrated an application that used confocal microscopy to form an optical tweezer by using objective lenses with NA>1 to highly focus laser light into a liquid to trap tiny particles. First, a sample was created on a glass slide with 100 µL of solution consisting of 10 mL H_2O/10 µL polystyrene beads. The ability to trap particles in solution allowed for the efficient demonstration of confocal Raman microscopy by using the high powered objective because the particle was forced to remain within the cross section to achieve single molecule Raman detection.

An attenuator was positioned in the optical path of each laser to reduce the optical intensity of the beams to prevent optical damage to sample particles from occurring. The optical density, OD, is related to transmission, T, by the two following equations: $OD = log_{10}(\frac{1}{10})$ and $T = 10^{-OD}$. The 700 mW infrared (1064 nm) laser was attenuated to 350 mW or 70 mW by using a selected neutral density filter that was mounted using a filter wheel and positioned in the optical path of only the trapping laser. The adjustable power, continuous wave visible (532 nm) laser was attenuated using a neutral density filter placed in the optical path of only the Raman laser before being focused through the dichroic mirror and overlapped with the trapping laser.

Then the Raman Tweezer setup was tested on the polystyrene bead sample polystyrene fluorescent orange, amine modified latex beads. The beads were of 2 micron diameter and were freely suspended in aqueous solution that was diluted by a factor of 1000. Placed slide on microscope and positioned camera to test trapping by visually observing fluorescence. Raman spectra was captured and shown above in Figure 5.4, Figure 5.5, and Figure 5.6 and serves as proof that this experiment successfully demonstrated trapping of objects. During this experiment photobleaching was observed in bead destruction from thermal effects of the laser. The higher the laser power, the quicker was damaged.

During the course of this experiment, gold was successfully trapped; however, the Raman spectrum of gold was unable to be measured because this setup lacked the proper wavelength laser (~730 nm). Prepared a solution by dissolving 1M KCl and Ag clusters in a 1:1 ratio and then mixed 0.1 mg bulk cytochrome c. Slide was prepared by adding 100 μL Ag/cytochrome c solution. Figure 5.7 and Figure 5.8 show the Raman spectra captured using only the green laser. Prepared a solution by dissolving 1M KCl and Ag clusters in a 1:1 ratio and prepared a slide using 100 μL of this solution. Loaded Ag aggregates with bulk cytochrome c by directly injected onto the hotspots of the Ag aggregates using XenoWorks Digital Microinjector. Figure 5.9 shows the Raman spectra of the loaded aggregates captured using only the green laser. These three figures of the Raman spectra of cytochrome c show an example of SERs using the Raman Tweezer setup.

7. Conclusion

When I initially joined this group, the lab was empty and my time here was mainly focused on developing this Raman Tweezer apparatus to demonstrate the feasibility of manipulating and controlling single particles and simultaneously performing Raman spectroscopy.

Localization of Raman measurement was achieved. Brownian motion was overcome by using the Raman Tweezer by trapping the particles of polystyrene beads suspended in solution and forcing them to remain within the cross section of the highly focused Raman laser An advantage of this setup is allowed for Raman spectra to be captured observing molecules in their natural environment. The molecules could remain suspended in solution and were not required to be attached to the glass surface unlike most SERs studies.

Continuing to explore new methods to improve the Raman Tweezer setup towards potential applications focused on single nanopore detection. Intensity of Rayleigh scattering is typically six orders of magnitude higher than that of Raman scattering. Need for experiments setups to filter Rayleigh scattering. The physical phenomenon of inherent, incessant motion of small particles suspended in a fluid known as *Brownian motion* requires increasing sensitivity of by improving the instrumentation used for Raman spectroscopy.

Nanopore sensing is an acceptable technique for detecting sizes of molecules; therefore, new measurement techniques can be developed by coupling Raman Tweezers and nanopore sensors to improve characterization methods during sample analysis. This work reported the successful construction of an optical trap and demonstrated simultaneous Raman detection on polystyrene

beads and Ag aggregates loaded with cytochrome c. More recent work has recently demonstrated on direct trapping of Ag nanoparticles. This shows promise for the potential applications after making further improvements to the Raman setup.

LIST OF REFERENCES

List of References

1. Ashkin, A, “Acceleration and Trapping of Particles by Radiation Pressure,” *Phys. Rev. Lett.* (1970) **24**, 4: 156-159.

2. Ashkin, A.; J. M. Dziedzic; J. E. Bjorkholm; and S. Chu, “Observation of a single-beam gradient force optical trap for dielectric particles,” *Opt. Lett.* (1986), **11**: 288-290.

3. Ashkin, A. “Forces of a single-beam gradient laser trap on a dielectric sphere in the ray optics regime,” *Biophys. J.* (1992), **61**: 569-582.

4. Ashkin, A. “Optical trapping and manipulation of neutral particles using lasers,” *Proc. Nat. Acad. Sci.* (1997) **94**, 4853-4860.

5. Nieminen, Timo A.; Gregor Knöner; Norman R. Heckenberg; and Halina Rubinsztein-Dunlop, "Physics of Optical Tweezers." *Laser Manipulation of Cells and Tissues*. Ed. Michael W. Berns and Karl Otto Greulich. Vol. 82. Amsterdam: Elsevier Academic Press, 2007. 207-36. Print. Methods in Cell Biology.

6. Wördemann, M. “Introduction to Optical Trapping.” *Structured Light Fields,* Berlin Heidelberg: Springer-Verlag, 2012. Print. Springer Ser. Springer Theses

7. Svoboda, K. and S.M. Block, “Biological Applications of Optical Forces,” *Annu. Rev. Biophys. Biomol. Struct.* (1994), **23**: 247-85.

8. Neuman, Keir C., and Steven M. Block, “Optical Trapping,” Review of Scientific Instruments (2004), **75**,9: 2787-2809.

9. Cherney, Daniel P. and Joel M. Harris, “Confocal Raman Microscopy of Optical-Trapped Particles in Liquids. *Annu. Rev. Anal. Chem.* (2010). **3**: 277-297

10. Bowman, Richard W and Miles J Padgett, “Optical trapping and binding,”

11. Novotny, Lukas; Hecht, Bert. *Principles of Nano-Optics*. 2nd ed. New York: Cambridge University Press, 2012. Print.

12. Zhang, Shu-Lin. *Raman Spectroscopy and its Application in Nanostructures*. Chichester, West Sussex: Wiley, 2012. Print.

13. Harris, Daniel C., and Michael D. Bertolucci. *Symmetry and Spectroscopy: An Introduction to Vibrational and Electronic Spectroscopy*. New York: Dover Publications, 1989. Print.

14. Dieing, Thomas; Olaf Hollricher; Jan Toporski, *Confocal Raman Microscopy*. Verlag Berlin Heidelberg Germany: Springer, 2010. Print.

15. Wolverson, Daniel. "Raman Spectroscopy." An Introduction to Laser Spectroscopy. Ed. David L. Andrews and Andrey A. Demidov. New York: Plenum, 1995. 91-114. Print.

16. Kneipp, Katrin; Martin Moskovits; Harald Kneipp, *Surface-Enhanced Raman Scattering: Physics and Applications*. Berlin: Springer, 2006. Print.

17. Everall, Neil J. "Industrial Applications of Raman Spectroscopy." An Introduction to Laser Spectroscopy. Ed. David L. Andrews and Andrey A. Demidov. New York: Plenum, 1995. 115-131. Print.